

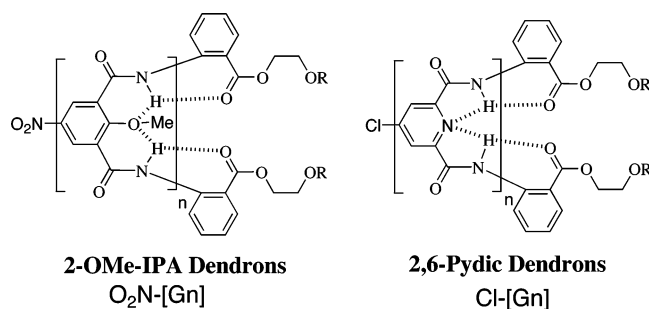
## A New Class of Intramolecularly Hydrogen-Bonded Dendrons Based on a 2-Methoxyisophthalamide Repeat Unit

Christopher J. Gabriel, Matthew P. DeMatteo, Noel M. Paul, Tomohisa Takaya, Terry L. Gustafson, Christopher M. Hadad,\* and Jon R. Parquette\*

Department of Chemistry, The Ohio State University, 100 West 18th Avenue, Columbus, Ohio 43210

hadad.1@osu.edu; parquett@chemistry.ohio-state.edu

Received June 29, 2006



The synthesis and conformational properties of folded dendrons based on a 2-methoxyisophthalamide (2-OMe-IPA) repeat unit are described. The hydrodynamic properties of dendrons preorganized via the *syn-syn* conformational preference of 2-methoxyisophthalamide are compared with 2,6-pyridinedicarboxamide (2,6-pydic) analogues. The effect of subtle differences in the nature of the conformational equilibria that exist within the 2-OMe-IPA and 2,6-pydic repeat units on the global structural properties of the corresponding dendrons was explored computationally, by <sup>1</sup>H-DOSY NMR spectroscopy and time-resolved fluorescence anisotropy (TRFA) measurements. Whereas the *syn-syn* preference of the 2-OMe-IPA branched repeat unit is stabilized entirely by intramolecular hydrogen-bonding interactions, this preference in the 2,6-pydic system is a consequence of both intramolecular hydrogen-bonding and dipole minimization effects. However, nonspecific solvophobic compression is more important in determining hydrodynamic properties than solvent-dependent shifts in the conformational equilibria of the repeat unit for both dendron series.

### Introduction

The allosteric conformational interconversions responsible for the modulation of function in proteins are highly dynamic processes involving multiple, correlated conformational equilibria that transmit local conformational perturbations to the global structure. Many of the applications and unique properties envisaged for dendrimers rely on an ability to control the three-dimensional organization of their structures over long length scales.<sup>1</sup> Accordingly, the nature of the conformational interplay that communicates localized variations in the structure or

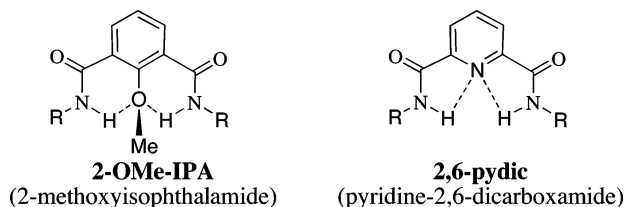
conformational equilibria to the global structure of a dendrimeric macromolecule is a crucial factor in the design of well-defined, three-dimensionally organized structures. Previous theoretical<sup>2</sup> and experimental<sup>3</sup> studies demonstrated that variations in macromolecular architecture have an impact on the physical and chemical properties of dendrimers in solution. For example, studies comparing dendrimers with their linear isomers revealed significant differences in hydrodynamic properties.<sup>4</sup> However, there are few studies directly evaluating the effect of localized shifts in the conformational equilibria of a structural subunit on the consequent global properties in solution. A recent study

(1) (a) Boas, U.; Heegaard, P. M. H. *Chem. Soc. Rev.* **2004**, *33*, 43. (b) Frechet, J. M. J. *J. Polym. Sci., Part A: Polym. Chem.* **2003**, *41*, 3713. (c) Balzani, V.; Ceroni, P.; Maestri, M.; Vicinelli, V. *Curr. Opin. Chem. Biol.* **2003**, *7*, 657. (d) Yokoyama, S.; Otomo, A.; Nakahama, T.; Okuno, Y.; Mashiko, S. *Top. Curr. Chem.* **2003**, *228*, 205. (e) Patri, A. K.; Majoros, I. J.; Baker, J. R. *Curr. Opin. Chem. Biol.* **2002**, *6*, 466. (f) Tomalia, D. A. *High Perform. Polym.* **2001**, *13*, S1.

(2) (a) Bosko, J. T.; Todd, B. D.; Sados, R. J. *J. Chem. Phys.* **2004**, *121*, 12050. (b) Lyulin, S. V.; Darinskii, A. A.; Lyulin, A. V.; Michels, M. A. J. *Macromolecules* **2004**, *37*, 4676. (c) Rosenfeldt, S.; Dingenouts, N.; Potschke, D.; Ballauff, M.; Berresheim, A. J.; Muellen, K.; Lindner, P. *Angew. Chem., Int. Ed.* **2004**, *43*, 109. (d) Ballauff, M.; Likos, C. N. *Angew. Chem., Int. Ed.* **2004**, *43*, 2998.

probing the effect of the local *trans* → *cis* photoisomerization of azobenzene dendron/core linkages on the corresponding hydrodynamic volumes observed comparatively small volume changes in dendrimers,<sup>5</sup> presumably due to the high segmental mobility that exists within dendrimers constructed with flexible bond connections.<sup>3c,6</sup>

We have recently developed a dendrimeric system that adopts a compact, helical conformation due to the *syn-syn* conformational preference of the pyridine-2,6-dicarboxamide (2,6-pydic) repeat unit.<sup>7</sup> The preorganized structure of the 2,6-pydic repeat unit appears to play a critical role in mediating the transfer of local perturbations to the dendrimer structure. For example, a 2,6-pydic dendrimer system exhibited large variations in hydrodynamic volumes upon relatively minor modifications of the dendron/core linkage.<sup>8a</sup> Although it is possible to envisage several potential, preorganized repeat units displaying a qualitatively similar conformational preference to that of the 2,6-pydic system, the ultimate effect of small variations in conformational equilibria of a dendritic subunit on the global properties of a dendrimer are not well understood. For example, 2-methoxyisophthalamide (2-OMe-IPA) represents a potential repeat unit that exhibits a *syn-syn* conformational preference analogous to the 2,6-pydic system and, therefore, might also serve as a preorganizing subunit for dendrimeric structures. However, the 2-OMe-IPA and 2,6-pydic systems differ in both the nature and the source of this conformational preference. Therefore, the goal of this work focuses on understanding how apparently minor differences in the conformational equilibria exhibited by these two potentially similar repeat units are manifested at the global hydrodynamic level.



## Results and Discussion

**Conformational Preference of 2-Methoxy-*N,N'*-diphenylisophthalamide.** Preorganization of the 2-OMe-IPA and 2,6-pydic dendrons capitalizes on the preference of these repeat units to exist predominantly in the *syn-syn* conformation. The structure of 2-methoxy-*N,N'*-diphenylisophthalamide, **1**, was optimized by density functional theory (DFT) at the B3LYP/6-31G\* level of theory,<sup>8</sup> and six unique conformations were located. These conformations corresponded to three *anti-anti* conformers differing in the relative orientation of the amide functions, one *syn-syn* conformer tilting the amide groups toward opposite faces, and two *syn-anti* conformers (see the Supporting Information). Single-point energy calculations were performed in the gas phase and using the PCM solvation model<sup>9</sup> with CHCl<sub>3</sub> and DMSO as the solvents at the B3LYP/6-311+G\*\* level of theory. The *syn-syn* conformation is preferred over the *syn-anti* conformation by 2.3 kcal/mol in the gas phase (Table 1). However, the preference for the *syn-syn* conformation decreases significantly as the polarity of the solvent increases. The *syn-syn* conformation of 2-OMe-IPA **1** is lowest in energy because this conformation permits intramolecular hydrogen-bonding interactions to occur between the amide NHs and the methoxy oxygen.<sup>10</sup> Accordingly, the solvent dependence of the *syn-syn* conformational preference is likely due to a disruption of the favorability of the intramolecular hydrogen-bonding interactions which stabilize this conformation. 2-Methoxy-*N,N'*-diphenylisophthalamide, **2**, was similarly optimized and resulted in six unique conformations which were virtually identical to those located for **1**. The absence of intramolecular hydrogen-bonding interactions affords a preference for the *anti-anti* configuration by 0.6 kcal/mol over the *syn-anti* conformation and by 1.5 kcal/mol over the *syn-syn* conformation. As the polarity of the solvent increases, the preference for the *anti-anti* conformation increases to the exclusion of all other conformations.

The charge distribution in the molecules was then determined by natural population analysis<sup>11</sup> at the B3LYP/6-311+G\*\* level of theory to ascertain the presence of hydrogen-bonding interactions (Figure 1). By examining the distribution of charge in these molecules, it is possible to examine the hydrogen-bonding or dipole–dipole interactions stabilizing any given conformation (see the Supporting Information for charge

(3) (a) Peerlings, H. W. I.; Trimbach, D. C.; Meijer, E. W. *Chem. Commun.* **1998**, 497. (b) Stancik, C. M.; Pople, J. A.; Trollis, M.; Lindner, P.; Hedrick, J. L.; Gast, A. P. *Macromolecules* **2003**, *36*, 5765. (c) Orlicki, J. A.; Viernes, N. O. L.; Moore, J. S.; Sendjarevic, I.; McHugh, A. J. *Langmuir* **2002**, *18*, 9990. (d) Jayakumar, K. N.; Bharathi, P.; Thayumanaavan, S. *Org. Lett.* **2004**, *6*, 2547. (e) Harth, E. M.; Hecht, S.; Helms, B.; Malmstrom, E. E.; Frechet, J. M. J.; Hawker, C. J. *J. Am. Chem. Soc.* **2002**, *124*, 3926. (f) Evmenenko, G.; Bauer, B. J.; Kleppinger, R.; Forier, B.; Dehaen, W.; Amis, E. J.; Mischenko, N.; Reynaers, H. *Macromol. Chem. Phys.* **2001**, *202*, 891. (g) Chen, Y.; Shen, Z.; Pastor-Perez, L.; Frey, H.; Stiriba, S.-E. *Macromolecules* **2005**, *38*, 227. (h) Gorman, C. B. *C. R. Chim.* **2003**, *6*, 911–918. (i) Chasse, T. L.; Yohannan, J. C.; Kim, N.; Li, Q.; Li, Z.; Gorman, C. B. *Tetrahedron* **2003**, *59*, 3853.

(4) (a) Stiriba, S.-E.; Kautz, H.; Frey, H. *J. Am. Chem. Soc.* **2002**, *124*, 9698. (b) Newkome, G. R.; Moorefield, C. N.; Epperson, J. D. *Eur. J. Org. Chem.* **2003**, 3666.

(5) (a) Junge, D. M.; McGrath, D. V. *J. Am. Chem. Soc.* **1999**, *121*, 4912. (b) Li, S.; McGrath, D. V. *J. Am. Chem. Soc.* **2000**, *122*, 6795. (c) Liao, L.-X.; Junge, D. M.; McGrath, D. V. *Macromolecules* **2002**, *35*, 319. (d) Liao, L.-X.; Stellacci, F.; McGrath, D. V. *J. Am. Chem. Soc.* **2004**, *126*, 2181. (e) Grebel-Koehler, D.; Liu, D.; De Feyter, S.; Enkelmann, V.; Weil, T.; Engels, C.; Samyn, C.; Muellen, K.; De Schryver, F. C. *Macromolecules* **2003**, *36*, 578. (f) Kumar, G. S.; Neckers, D. C. *Chem. Rev.* **1989**, *89*, 1915.

(6) (a) Maiti, P. K.; Cagin, T.; Wang, G.; Goddard, W. A., III. *Macromolecules* **2004**, *37*, 6236. (b) Adhiya, A.; Wesdemiotis, C. *Int. J. Mass Spectrom.* **2002**, *214*, 75–88. (c) Cameron, C. S.; Gorman, C. B. *Adv. Funct. Mater.* **2002**, *12*, 17–20.

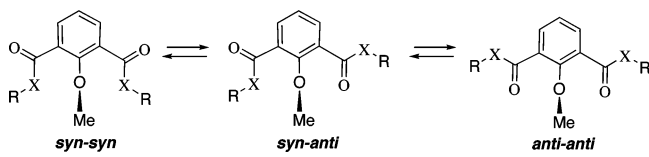
(7) (a) Parquette, J. R. *C. R. Chim.* **2003**, *6*, 779. (b) Huang, B.; Prantil, M. A.; Gustafson, T. L.; Parquette, J. R. *J. Am. Chem. Soc.* **2003**, *125*, 14518. (c) Huang, B.; Parquette, J. R. *J. Am. Chem. Soc.* **2001**, *123*, 2689. (d) Recker, J.; Tomcik, D. J.; Parquette, J. R. *J. Am. Chem. Soc.* **2000**, *122*, 10298. (e) Huang, B.; Parquette, J. R. *Org. Lett.* **2000**, *3*, 239.

(8) (a) Frisch, M. J. Gaussian 03, Revision B.04, Gaussian, Inc.; Pittsburgh, PA, 2003. (b) Becke, A. D. *J. Chem. Phys.* **1993**, *98*, 5648. (c) Lee, C.; Yang, W.; Parr, R. G. *Phys. Rev. B* **1988**, *37*, 785. (d) Hehre, W. J.; Radom, L.; Schleyer, P. v. R.; Pople, J. A. *Ab Initio Molecular Orbital Theory*; John Wiley & Sons: New York, 1986.

(9) (a) Miertus, S.; Scrocco, E.; Tomasi, J. *Chem. Phys.* **1981**, *55*, 117. (b) Cammi, R.; Tomasi, J. *J. Comput. Chem.* **1995**, *16*, 1449. (c) Tomasi, J.; Persico, M. *Chem. Rev.* **1994**, *94*, 2027.

(10) For examples of two- and three-centered hydrogen bonding to a methoxy group, see: (a) Wu, Z.-Q.; Jiang, X.-K.; Zhu, S.-Z.; Li, Z.-T. *Org. Lett.* **2004**, *6*, 229. (b) Zhu, J.; Wang, X.-Z.; Chen, Y.-Q.; Jiang, X.-K.; Chen, X.-Z.; Li, Z.-T. *J. Org. Chem.* **2004**, *69*, 6221. (c) Gong, B.; Zeng, H.; Zhu, J.; Yuan, L.; Han, Y.; Cheng, S.; Furukawa, M.; Parra, R. D.; Kovalevsky, A. Y.; Mills, J. L.; Skrzypczak-Jankun, E.; Martinovic, S.; Smith, R. D.; Zheng, C.; Szyperski, T.; Zeng, X. C. *Proc. Natl. Acad. Sci. U.S.A.* **2002**, *99*, 11583. (d) Zeng, H.; Miller, R. S.; Flowers, R. A., II; Gong, B. *J. Am. Chem. Soc.* **2000**, *122*, 2635. (e) Hamuro, Y.; Geib, S. J.; Hamilton, A. D. *J. Am. Chem. Soc.* **1996**, *118*, 7529.

(11) (a) Reed, A. E.; Weinstock, R. B.; Weinhold, F. *A. J. Chem. Phys.* **1985**, *83*, 735. (b) Reed, A. E.; Curtiss, L. A.; Weinhold, F. *Chem. Rev.* **1988**, *88*, 899.

**TABLE 1.** Relative Energies and Dipole Moments of **1** and **2** at the B3LYP/6-311+G\*\*//B3LYP/6-31G\* Level of Theory<sup>a,b</sup>


The figure shows three chemical structures representing different conformations of a molecule with a central pyridine ring and two amide groups. The first structure is labeled 'syn-syn', the second 'syn-anti', and the third 'anti-anti'. Each structure shows the relative orientation of the amide groups and the methoxy group on the pyridine ring. Equilibrium arrows connect the structures.

X = NH ( <b>1</b> )	<b>1</b> <i>syn-syn</i>	<b>1</b> <i>syn-anti</i>	<b>1</b> <i>anti-anti</i>
$\Delta G_{\text{rel}}$ (298 K) (gas phase)	0.0	2.3	4.6
$\Delta E_{\text{rel}}$ (PCM, CHCl <sub>3</sub> )	0.0	1.3	3.1
$\Delta E_{\text{rel}}$ (PCM, DMSO)	0.0	0.9	1.6
$\mu$ (gas phase)	3.3	3.3	5.5
$\mu$ (CHCl <sub>3</sub> )	4.3	4.1	7.1
$\mu$ (DMSO)	4.7	4.4	8.0
X = O ( <b>2</b> )	<b>2</b> <i>syn-syn</i>	<b>2</b> <i>syn-anti</i>	<b>2</b> <i>anti-anti</i>
$\Delta G_{\text{rel}}$ (298 K) (gas phase)	1.5	0.6	0.0
$\Delta E_{\text{rel}}$ (PCM, CHCl <sub>3</sub> )	2.3	1.3	0.0
$\Delta E_{\text{rel}}$ (PCM, DMSO)	2.7	1.6	0.0
$\mu$ (gas phase)	2.4	1.3	3.1
$\mu$ (CHCl <sub>3</sub> )	2.8	1.6	3.8
$\mu$ (DMSO)	2.9	1.8	4.2

<sup>a</sup> Energy given in kcal/mol. <sup>b</sup> Dipole moment ( $\mu$ ) in Debye.

distribution diagrams). Upon examining the atomic charges of **1**, it is apparent that there are hydrogen-bonding interactions between the amide hydrogens and the methoxy oxygen in the *syn-syn* and *syn-anti* conformations. This would appear to explain the preference for the *syn-syn* conformation in the various solvents and the fact that the *syn-anti* conformation is the next most favorable conformation. Structure **2**, on the other hand, does not have the capability for hydrogen bonding, and as such, the charge distribution is similar for all conformations.

Analysis of the calculated dipole moments shows that the preferred energy minimum does not strictly correlate with changes in dipole moment. The *syn-syn* and *syn-anti* conformations of **1** appear to have very similar dipole moments, but this trend does not correlate with the energetic preference for the *syn-syn* conformation, contrasting with *N,N'*-diphenylpyridine-2,6-dicarboxamide, **3** (vide infra). The diester **2** displays a preference for the *anti-anti* conformation which has the largest dipole moment. This preference in the gas phase is likely a consequence of steric interactions between the methoxy function and the ester groups encountered in the *syn-syn* conformation. The increased energetic preference for the *anti-anti* conformation as the polarity of the solvent increases can be attributed to the higher dipole moment.

**Conformational Preference of *N,N'*-Diphenylpyridine-2,6-dicarboxamide.** Optimization of *N,N'*-diphenylpyridine-2,6-dicarboxamide, **3**, at the B3LYP/6-31G\* level of theory revealed four unique conformations. These conformations corresponded to two different *anti-anti* conformers with the carboxamide groups tilted slightly toward the same face of the pyridine ring and to opposite faces, one planar *syn-syn* conformer and one *syn-anti* conformer. The ester variant **4** afforded five unique conformations corresponding to two *anti-anti* conformers, two *syn-syn* conformations, and one *syn-anti* orientation.

In contrast to **1** and **2**, which display preferences for the *syn-syn* and *anti-anti* conformations, respectively, both **3** and **4** prefer the *syn-syn* conformation in the gas phase (Table 2). However, **3** prefers the *syn-syn* orientation over *syn-anti* by 6.3 kcal/mol, whereas **4**, which lacks the potential for stabilizing hydrogen-bonding interactions, prefers the *syn-syn* orientation by 1.0

kcal/mol. Likewise, **3** demonstrates a 10 kcal/mol preference for *syn-syn* over *anti-anti*, whereas **4** has only a 2 kcal/mol preference. As the polarity of the solvent increases, the preference for the *syn-syn* conformation in both cases decreases significantly. The preference for the *syn-syn* over the *anti-anti* conformation in **3** remains virtually unchanged by solvent. However, the preference for *syn-syn* over *syn-anti* conformations decreases significantly from 6.3 kcal/mol in the gas phase to 3.9 kcal/mol in DMSO. Compound **4** exhibits a similar trend, but the preference for *syn-syn* over *syn-anti* remains virtually unchanged, whereas the preference in DMSO shifts from *syn-syn* to *anti-anti*. It is also worthy of note that in more polar solvents, the preference for any one conformation becomes very small (less than 1 kcal/mol) in compound **4** in contrast to **3**.

Although the preference for the *syn-syn* conformation is less favored in the 2-methoxyisophthalamide unit (2-OMe-IPA) in comparison with the pyridine-2,6-dicarboxamide (2,6-pydic) system, the relative energetics are qualitatively similar. However, intramolecular hydrogen bonding appears to play a more important role in determining the conformational preference of 2-methoxyisophthalamides, as compared with the pyridine-2,6-dicarboxamides. Accordingly, in contrast to **1** and **2**, the decrease in relative energy of the conformers in **3** and **4** generally correlates with a decrease in the corresponding calculated dipole moments. Therefore, intramolecular hydrogen bonding plays a more important role than dipole moment minimization in determining the conformational preference of 2-methoxyisophthalamides, as compared with the pyridine-2,6-dicarboxamides. Accordingly, polar aprotic solvents that interfere with intramolecular hydrogen-bonding interaction would be more likely to shift the conformational preference of 2-OMe-IPA dendrons than for the 2,6-pydic congeners.

**Synthesis of 2-OMe-IPA and 2,6-Pydic Dendrons.** 2-Methoxy-5-nitroisophthaloyl dichloride,<sup>12</sup> **7**, prepared from 2,6-dimethylanisole as shown in Scheme 1, was selected to serve as the branched repeat unit for the 2-OMe-IPA dendron synthesis. Condensation of tetraethylene glycol monomethyl ether with isatoic anhydride in dioxane at 75 °C provided the terminal anthranilate building block (**9**) in 88% yield. Tetraethylene glycol was incorporated at the termini because of the known ability of poly(ethylene glycol) moieties to impart solubility in a variety of solvents.<sup>13</sup>

The dendrons were constructed via a convergent synthetic protocol, whereby generational growth was achieved using amide bond formation reactions of diacid chloride **7** and focal activation was achieved by SnCl<sub>2</sub> reduction of the nitro group (Scheme 2). Accordingly, amide bond formation between **7** and **9** provided O<sub>2</sub>N-[G1] **10** in 82% yield. SnCl<sub>2</sub> reduction of **10** followed by reaction with **7** afforded O<sub>2</sub>N-[G2] **11**, which was elaborated to O<sub>2</sub>N-[G3] **12** following the same protocol. Characterization with regard to molecular weight, structure, and dispersity was accomplished by electrospray ionization or MALDI-TOF MS, NMR, and SEC analysis (Supporting Information), respectively.

**Solid-State Structure of 2-OMe-IPA G1 Dendron.** A clear, colorless crystal (monoclinic, space group P1) of chiral dendron H<sub>2</sub>N-[G1] **13** was obtained by slow evaporation from a mixture of CHCl<sub>3</sub> and hexane. X-ray diffraction showed that the asymmetric unit was composed of two molecules of opposite

(12) Chapoteau, E.; Chowdhary, M. S.; Czech, B. P.; Kumar, A.; Zazulak, W. J. *Org. Chem.* **1992**, *57*, 2804.

(13) Stone, M. T.; Moore, J. S. *Org. Lett.* **2004**, *6*, 469.



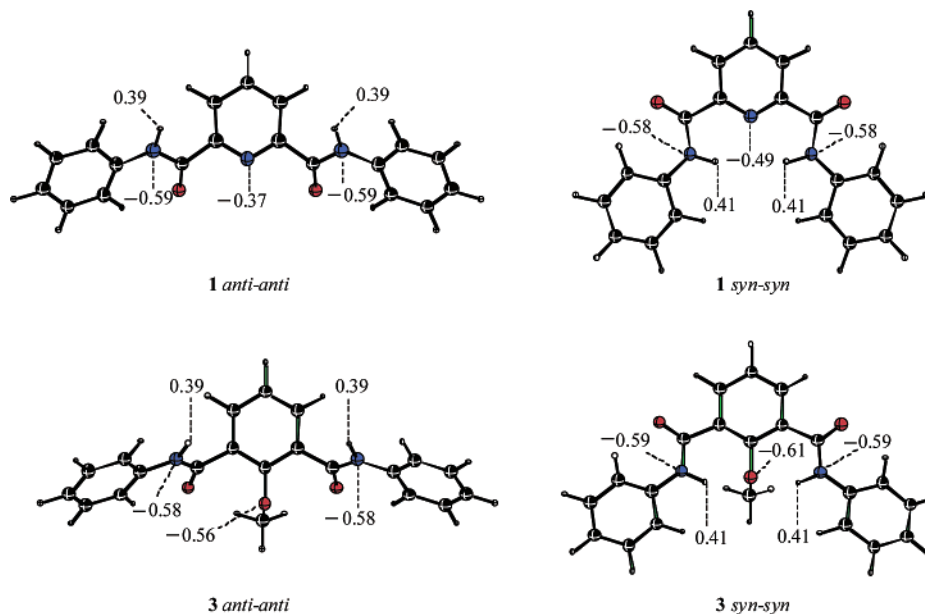


**FIGURE 1.** Natural population analysis of repeat units **1** and **3** at the B3LYP/6-311+G\*\*//B3LYP/6-31G\* level of theory. All charges are in units of electrons.

**TABLE 2.** Relative Energies and Dipole Moments of **3** and **4** at the B3LYP/6-311+G\*\*//B3LYP/6-31G\* Level of Theory<sup>a,b</sup>

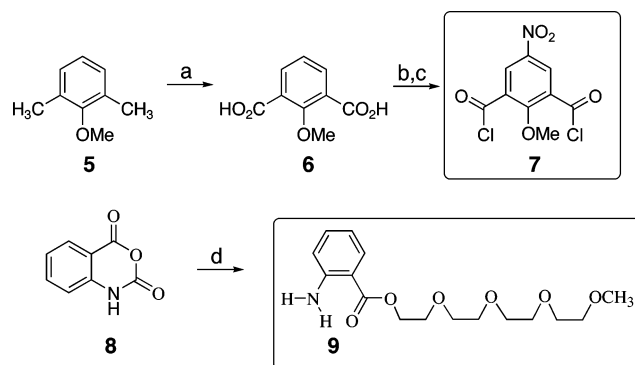
X = NH ( <b>3</b> )	<b>3</b> <i>syn-syn</i>	<b>3</b> <i>syn-anti</i>	<b>3</b> <i>anti-anti</i>
$\Delta G_{\text{rel}}$ (298 K) (gas phase)	0.0	6.3	10.1
$\Delta E_{\text{rel}}$ (PCM, CHCl <sub>3</sub> )	0.0	4.8	12.6
$\Delta E_{\text{rel}}$ (PCM, DMSO)	0.0	3.9	10.1
$\mu$ (gas phase)	1.2	5.0	6.8
$\mu$ (CHCl <sub>3</sub> )	1.6	6.2	8.6
$\mu$ (DMSO)	1.8	6.8	9.5
X = O ( <b>4</b> )	<b>4</b> <i>syn-syn</i>	<b>4</b> <i>syn-anti</i>	<b>4</b> <i>anti-anti</i>
$\Delta G_{\text{rel}}$ (298 K) (gas phase)	0.0	1.0	2.1
$\Delta E_{\text{rel}}$ (PCM, CHCl <sub>3</sub> )	0.0	1.0	0.4
$\Delta E_{\text{rel}}$ (PCM, DMSO)	0.7	1.5	0.0
$\mu$ (gas phase)	0.1	3.1	5.3
$\mu$ (CHCl <sub>3</sub> )	0.1	3.8	6.6
$\mu$ (DMSO)	0.2	4.2	7.3

<sup>a</sup> Energy given in kcal/mol. <sup>b</sup> Dipole moment ( $\mu$ ) in Debye.

helical sense that exhibited the predicted *syn-syn* conformation relating the carboxamides (Figure 2). Three-center hydrogen-bonding interactions of the carboxamide N–Hs with the 2-methoxy oxygen ( $d_{\text{N-H}\cdots\text{O-Me}}$  2.345 and 2.016 Å) and the ester carbonyl oxygens ( $d_{\text{N-H}\cdots\text{O=}}$  2.099 and 2.104 Å) stabilize the *syn-syn* conformation. The differences in the hydrogen-bond distances are a consequence of the lack of 2-fold symmetry in the approximately helical conformation relating the terminal anthranilates, which is reflected in the deviation of one of the two carboxamide carbonyls from coplanarity with the isophthalamide ring by 39.30°.

**Solution-State Structure.** <sup>1</sup>H NMR and IR spectral data were in good agreement with the presence of intramolecular hydrogen bonding throughout the dendron structure in solution for both systems (Table 3). Large downfield shifts of the amide N–Hs, similar to those observed for the pyridine-2,6-dicarboxamide

**SCHEME 1.** Synthesis of Dendron Building Blocks<sup>a</sup>

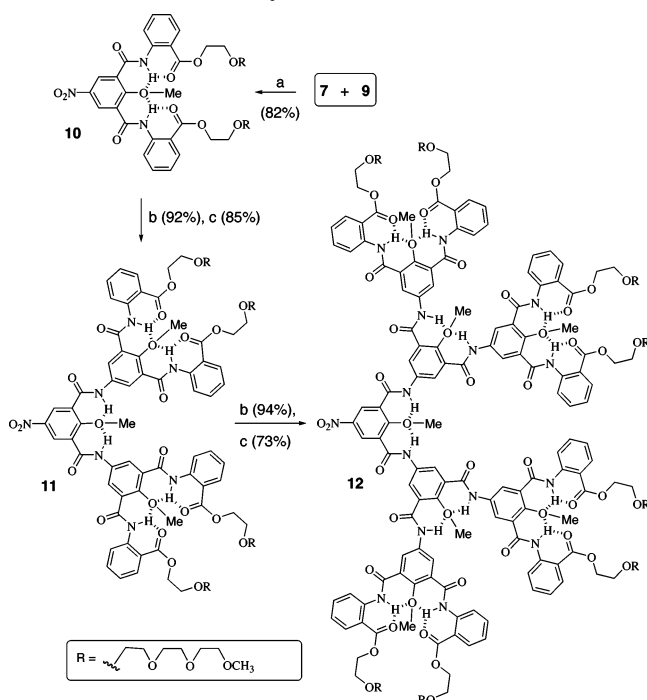


<sup>a</sup> Key: (a) KMnO<sub>4</sub>, H<sub>2</sub>O, 64%; (b) HNO<sub>3</sub>–H<sub>2</sub>SO<sub>4</sub>, H<sub>2</sub>O, 0 °C, 88%; (c) (COCl)<sub>2</sub>, CH<sub>2</sub>Cl<sub>2</sub>, DMF (cat.), quant; (d) tetraethyleneglycol monomethyl ether, DMAP, dioxane, 75 °C, 88%.

dendrons, occurred for all 2-OMe-IPA dendrons. The infrared spectra in CDCl<sub>3</sub> of **10–12** exhibited broad N–H stretching bands at 3256–3367 cm<sup>−1</sup> characteristic of hydrogen-bonded N–H groups and similar to the 2,6-pydic systems.<sup>7c</sup>

The conformational preferences of the 2,6-pydic and 2-OMe-IPA dendrons were investigated in CDCl<sub>3</sub> by 2D NOESY <sup>1</sup>H NMR spectroscopy. 2-OMe-IPA dendrons **10** and **11** revealed NOE cross-peaks between the amide NH protons and both the methoxyl and aromatic protons. These close contacts are consistent with the occurrence of both the *syn-syn* and *syn-anti* forms in the conformational ensemble, as predicted computationally (Figure 3). However, no cross-peaks indicating close contacts between the amide NHs and the pyridyl ring protons were observed for 2,6-pydic dendrons **14** or **15**, consistent with a greater *syn-syn* conformational preference.

**Comparison of Hydrodynamic Properties.** The DFT studies suggest that the *syn-syn* conformation is stabilized primarily via hydrogen-bonding interactions in the 2-OMe-IPA system, whereas both dipole minimization and hydrogen bonding play a role in the 2,6-pydic system (vide supra). This difference affords the 2,6-pydic system a capacity to remain in a compact

SCHEME 2. Dendron Synthesis<sup>a</sup>

<sup>a</sup> Key: (a) DMAP (cat.) CH<sub>2</sub>Cl<sub>2</sub>–pyr; (b) SnCl<sub>2</sub>·2H<sub>2</sub>O, EtOAc–MeOH, reflux; (c) **3**, DMAP (cat.) CH<sub>2</sub>Cl<sub>2</sub>–pyr.

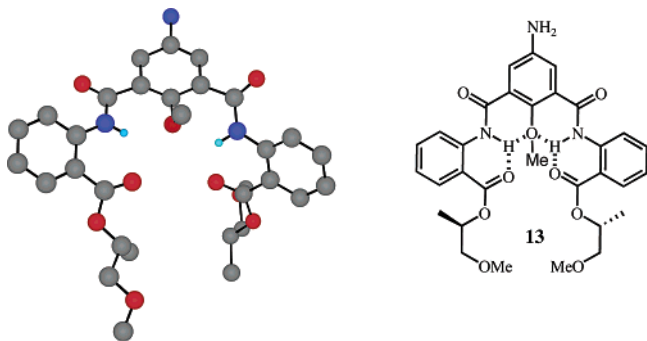


**FIGURE 2.** X-ray crystal structure of H<sub>2</sub>N-[G1] dendron (**13**) indicating a *syn-syn* conformational preference in the solid state. Hydrogens have been omitted on the left structure for clarity.

**TABLE 3.** <sup>1</sup>H NMR Resonances of Amide N–Hs (ppm)<sup>a</sup>

dendron	CDCl <sub>3</sub>			DMSO- <i>d</i> <sub>6</sub>		
	NH <sub>a</sub>	NH <sub>b</sub>	NH <sub>c</sub>	NH <sub>a</sub>	NH <sub>b</sub>	NH <sub>c</sub>
O <sub>2</sub> N-[G1] ( <b>10</b> )	11.95			11.49		
O <sub>2</sub> N-[G2] ( <b>11</b> )	11.82	9.69		11.53	11.01	
O <sub>2</sub> N-[G3] ( <b>12</b> )	11.83	9.78	9.78	11.53	10.84	10.97
Cl-[G1] ( <b>14</b> )	12.65			12.44		
Cl-[G2] ( <b>15</b> )				12.45	11.63	
Cl-[G3] ( <b>16</b> )				12.43	11.67	11.45

<sup>a</sup> H<sub>a</sub> = third shell (terminal); H<sub>b</sub> = second shell; H<sub>c</sub> = first shell (focal).

folded state in aqueous media.<sup>14</sup> In contrast, the conformational properties of 2-OMe-IPA could be expected to exhibit more sensitivity to polar solvents such as MeOH or DMSO that potentially disrupt hydrogen-bonding interactions. We reasoned that the greater solvent sensitivity of *syn-syn* preference in the

(14) Hofacker, A. L.; Parquette, J. R. *Angew. Chem., Int. Ed.* **2005**, *44*, 1053.

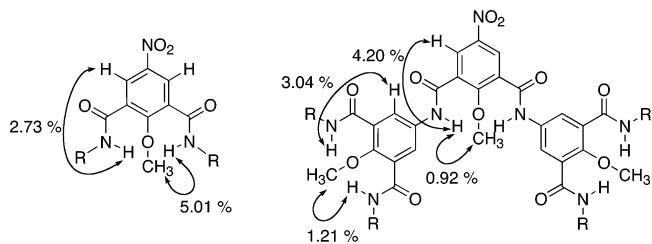


**FIGURE 3.** NOESY enhancements (500 MHz, CDCl<sub>3</sub>, 27 °C) of O<sub>2</sub>N-[G1] (**10**) and O<sub>2</sub>N-[G2] (**11**).

2-OMe-IPA system might be expressed as an increase in hydrodynamic volume in polar solvents.

Accordingly, the effect of solvent on the hydrodynamic volumes of the 2-OMe-IPA dendrons (**10–12**) was compared with analogous 2,6-pyridic dendrons (**14–16**) displaying identical tetraethyleneglycol terminal esters. Dendrons **14–16** were constructed from anthranilate **7** and 4-chloropyridine-2,6-dicarbonyl chloride following an analogous generational growth protocol we previously reported for related pentaethyleneglycol terminated 2,6-pyridic systems.<sup>14</sup> Comparison of the hydrodynamic volume ( $V_{\text{hyd}}$ ) of 2-OMe-IPA dendron **10**, measured by DOSY-NMR spectroscopy,<sup>15</sup> relative to the calculated van der Waals volume<sup>16</sup> ( $V_{\text{vdw}}$ ), indicated that the  $V_{\text{hyd}}$  of the dendron was similarly compact in CDCl<sub>3</sub> and CD<sub>3</sub>OD, but significantly expanded in DMSO-*d*<sub>6</sub> (Figure 4 and Supporting Information). This structural expansion may have occurred, in part, due to disruption of the intramolecular hydrogen-bonding interactions by DMSO-*d*<sub>6</sub>. In contrast, the structure of 2,6-pyridic dendron **14** was compact in all three solvents, slightly decreasing in  $V_{\text{hyd}}$  going from CDCl<sub>3</sub> → CD<sub>3</sub>OD → DMSO-*d*<sub>6</sub>. The differential sensitivity of the  $V_{\text{hyd}}$  of **10** and **14** aligns with the DFT-predicted local conformational behavior of the 2-OMe-IPA and 2,6-pyridic repeat units, respectively.

Determination of the hydrodynamic properties of dendrons **11–12** and **15–16** by DOSY-NMR spectroscopy was complicated by aggregation that occurred at the millimolar concentrations required for the NMR measurement. The presence of aggregated states in CD<sub>3</sub>OD, CDCl<sub>3</sub>, and DMSO-*d*<sub>6</sub> at millimolar concentrations was evident in highly broadened <sup>1</sup>H NMR spectra and the particularly large  $V_{\text{hyd}}/V_{\text{vdw}}$  ratios measured by DOSY-NMR (see the Supporting Information). Accordingly, to circumvent aggregation, the molecular dimensions of dendrons **11–12** and **15–16** were measured at submicromolar concentrations by time-resolved fluorescence anisotropy (TRFA) measurements<sup>17,18</sup> using the time-correlated single-photon counting method (TCSPC).<sup>19</sup> The samples were then diluted in this concentration range until the measured dimensions remained constant to ensure the presence of a monomolecular species in

(15) Young, J. K.; Baker, G. R.; Newkome, G. R.; Morris, K. F.; Johnson, C. S. *J. Macromolecules* **1994**, *27*, 3464.

(16) Calculated using Edward's increments: Edward, J. T. *J. Chem. Educ.* **1970**, *47*, 261.

(17) Fleming, G. R. *Chemical Applications of Ultrafast Spectroscopy*; Oxford University Press: New York, 1986.

(18) For examples of time-resolved fluorescence depolarization studies on dendrimers, see: (a) De Backer, S.; Prinzie, Y.; Verheijen, W.; Smet, M.; Desmedt, K.; Dehaen, W.; De Schryver, F. C. *J. Phys. Chem A* **1998**, *102*, 5451. (b) Hofkens, J.; Latterini, L.; De Belder, G.; Gensch, T.; Maus, M.; Vosch, T.; Karni, Y.; Schweitzer, G.; De Schryver, F. C.; Hermann, A.; Mullen, K. *Chem Phys. Lett.* **1999**, *304*, 1. Matos, M. S.; Hofkens, J.; Verheijen, W.; De Schryver, F. C.; Hecht, S.; Pollak, K. W.; Frechet, J. M. J.; Foreir, B.; Dehaen, W. *Macromolecules* **2000**, *33*, 2967.

(19) Buterbaugh, J. S.; Toscano, J. P.; Weaver, W. L.; Gord, J. R.; Hadad, C. M.; Gustafson, T. L.; Platz, M. S. *J. Am. Chem. Soc.* **1997**, *119*, 3580.

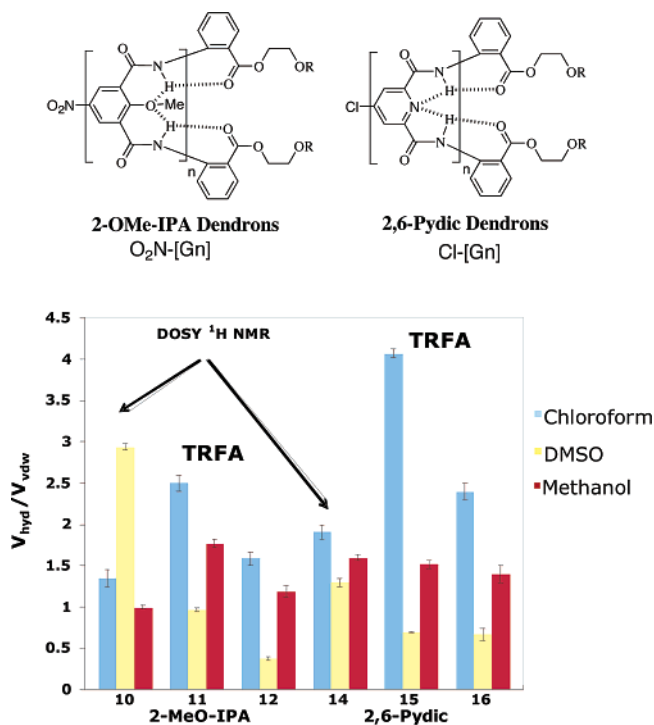


**FIGURE 4.** Packing efficiency ( $V_{\text{hyd}}/V_{\text{vdw}}$ ) as a function of generation and solvent for 2,6-pydic and 2-OMe-IPA dendrons. Hydrodynamic volumes measured by <sup>1</sup>H-DOSY NMR ( $10^{-3}$  M) for **10** and **14** and by TRFA ( $10^{-5}$ – $10^{-7}$  M) for **11**, **12**, **15**, and **16**.

solution.<sup>20</sup> The fluorescence anisotropy decays showed a biexponential profile consisting of a fast and a slow depolarization component (see the Supporting Information). The fast decay component likely represented an intramolecular energy-transfer depolarization process,<sup>21</sup> consistent with the presence of a delocalized excited state, whereas the slow component corresponded to the global rotation of the molecule. The hydrodynamic volumes ( $V_{\text{hyd}}$ ) were then calculated using the values of the rotational correlation times ( $\Theta_2$ ) via the Debye–Stokes–Einstein relation (DSE) as reported previously.<sup>7b</sup>

The hydrodynamic volumes of second- and third-generation 2,6-pydic and the 2-OMe-IPA dendrons displayed similar solvent dependencies that were different from first-generation 2-OMe-IPA dendron **10**. Generally, with the exception of **10**, all dendrons exhibited a maximal  $V_{\text{hyd}}$  in  $\text{CDCl}_3$  that progressively collapsed in the order  $\text{CDCl}_3 > \text{CD}_3\text{OD} > \text{DMSO-}d_6$ . This trend suggests that at higher generations, nonspecific solvophobic compression is more important in determining hydrodynamic properties than solvent-dependent shifts in the conformational equilibria of the repeat unit. The observed  $V_{\text{hyd}}$  compression correlates with apparent solvent quality, as evidenced by the qualitative observation that the dendrons tend to be more soluble in  $\text{CDCl}_3$  than either  $\text{CD}_3\text{OD}$  or  $\text{DMSO-}d_6$ . The similarity of the trends for both dendrons reflects the dominance of the tetraethyleneglycol termini in determining solubility characteristics. These solvent trends are congruent with the tendency of other dendrimer systems to collapse in poor solvents and expand in good solvents.<sup>22</sup>

(20) For use of the TRFA technique in 2,6-pydic dendrimers, see ref 7b.

(21) See ref 7b and: Tande, B. M.; Wagner, N. J.; Mackay, M. E.; Hawker, C. J.; Jeong, M. *Macromolecules* **2001**, *34*, 8580.

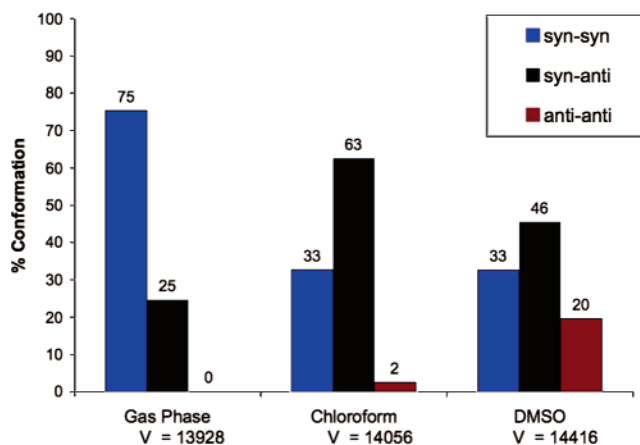


**FIGURE 5.** Calculated volume ( $\text{cm}^3/\text{mol}$ ) and percent contribution of *syn-syn* (ss), *syn-anti* (sa), and *anti-anti* (aa) conformations as a function of dielectric field in conformations with  $\sim 12$  kcal/mol of the global minimum for 2-OMe-IPA repeat unit in **11**.

**Monte Carlo Conformational Analysis of 2-OMe-IPA and 2,6-Pydic Second-Generation Dendrons.** To evaluate the potential of localized conformational changes to perturb the hydrodynamic volumes ( $V_{\text{hyd}}$ ) of the 2-OMe-IPA and 2,6-pydic systems relative to solvent quality, Monte Carlo conformational analysis of model second-generation dendrons **11** and **15** was performed using the AMBER\* force field.<sup>23</sup> These simulations only estimate the dielectric effect of the solvent and do not include any explicit solvent–solute interactions; therefore, they provide some guidance on the relative magnitude of the effect of intimate interactions between the dendron and the solvent when compared to experiment. The  $\text{NO}_2$  group in **11** was replaced by an H, and similarly, the Cl group in **15** was replaced by an H. The Monte Carlo multiple minimum search protocol<sup>24</sup> generated 100 000 starting conformers, which were subsequently optimized with the AMBER\* force field for the gas phase and also in the presence of  $\text{CHCl}_3$  and DMSO dielectric fields. Unique conformers within  $\sim 12$  kcal/mol of the global minimum were further analyzed at the HF/6-31G\* level of theory to calculate their volumes using the Gaussian suite of programs.<sup>8</sup> The Boltzmann contribution, calculated from the AMBER\* relative energies of each conformer, was then applied to the calculated volumes, and these Boltzmann-weighted volumes were summed to provide a conformationally averaged overall volume of the structure. The molar volumes were then correlated with geometrical trends of the corresponding shifts in the equilibria interconverting the *syn-syn*, *syn-anti*, and *anti-anti* conformations of the repeat unit that contribute to the conformational ensemble.

As shown in Figure 5, the calculated volumes of **11** increased slightly ( $\sim 4\%$ ) going from the gas phase  $\rightarrow \text{CHCl}_3 \rightarrow \text{DMSO}$ , in contrast with the experimental observation that the  $V_{\text{hyd}}$  (Table 4) was significantly larger in  $\text{CHCl}_3$  than in DMSO. The

(22) Bosman, A. W.; Janssen, H. M.; Meijer, E. W. *Chem. Rev.* **1999**, *99*, 1665.

(23) The Monte Carlo Multiple Minimum search protocol was used to generate 100 000 conformers of **11** and **15**. These conformers were then optimized under the AMBER\* force field for gas phase,  $\text{CHCl}_3$ , and DMSO dielectric fields. Structures within  $\sim 12$  kcal/mol of the global minimum after optimization were tabulated.

(24) As implemented in Macromodel 8.1, see: Mohamadi, F.; Richards, N. G. J.; Guida, W. C.; Liskamp, R.; Lipton, M.; Caufield, C.; Chang, G.; Hendrickson, T.; Still, W. C. *J. Comput. Chem.* **1990**, *11*, 440.

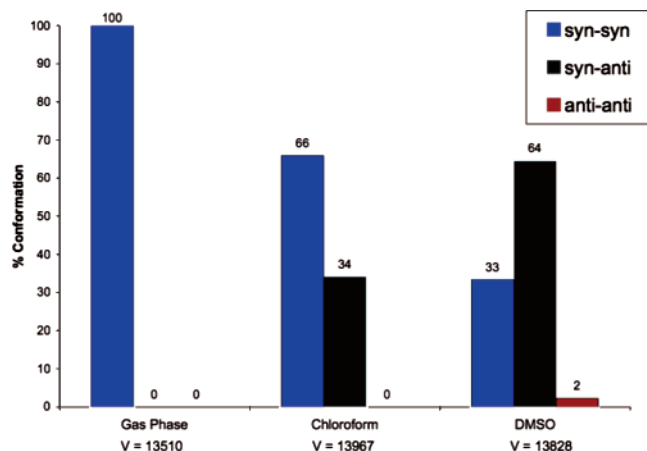


**FIGURE 6.** Calculated volume (cm<sup>3</sup>/mol) and percent contribution of *syn-syn* (ss), *syn-anti* (sa), and *anti-anti* (aa) conformations as a function of dielectric field in conformations within ~12 kcal/mol of the global minimum for 2,6-pydic repeat unit in **15**.

expansion in calculated volume occurred in conjunction with a shift in equilibria of the branched repeat unit from predominantly *syn-syn* in the gas phase (75ss/25sa/0aa) to predominately *syn-anti* in the presence of applied dielectric fields for CHCl<sub>3</sub> (33ss/63sa/2aa) and DMSO (33ss/46sa/20aa). These observations suggest that the 2-OMe-IPA system would expand slightly in solvents with high dielectric constants that can disrupt the intramolecular hydrogen bonding that stabilizes the *syn-syn* conformation in favor of the *syn-anti* and *anti-anti* forms. However, these computational results are not consistent with the experimental observations by TRFA methods. Since the experimental situation includes both the dielectric effect of the solvent as well as consideration of the intimate interactions between the dendron and the hydrogen-bonding solvent, these intimate interactions must be dramatically more important than

the dielectric effect alone. Furthermore, we should also note that the calculated change in volume is small (on the order of <5%), whereas the experimental change from CHCl<sub>3</sub> to DMSO is about a factor of 3.

In contrast to the gas-phase structure of the 2-OMe-IPA dendron, the conformational ensemble that comprises the global structure of the 2,6-pydic dendron **15** was composed of repeat units existing exclusively in the *syn-syn* conformation (Figure 6). Similar to 2-OMe-IPA **11**, the conformational equilibria shift increasingly toward the *syn-anti* conformation as the polarity increases going from CHCl<sub>3</sub> (66ss/34sa/0aa) to DMSO (33ss/64sa/2aa), but to a lesser extent. Moreover, the *anti-anti* conformation contributes much less to the equilibrium, even in DMSO, in which only 2% of the repeat units exist in the *anti-anti* form.

This local conformational change in the repeat unit is accompanied by an increase in the calculated volume similar to 2-OMe-IPA **11**, compared with the gas phase. However, both computational and experimental data indicate that the volume of 2,6-pydic **15** decreases slightly upon changing solvents from CHCl<sub>3</sub> to DMSO, contrasting with the calculated behavior of 2-OMe-IPA **11**. Comparison of the calculated structures of **11** and **15** reveals that whereas the percentage of the *anti-anti* form in **11** increases to 20% in DMSO, its contribution to the structure of **15** is negligible. A closer inspection of the computational structures that contribute to the ensemble below ~12 kcal/mol for **11** and **15** indicated that the focal shell repeat unit always adopts the *syn-syn* conformation, which causes nearly every peripheral position to exist in the *syn-anti* form. This arrangement appears to pack more efficiently than when both *syn-anti* and *syn-syn* forms coexist at the periphery of the dendrons in CHCl<sub>3</sub> (Figure 7). Because the conformational equilibria of 2,6-pydic repeat units exhibits little solvent dependence, the hydrodynamic volumes are dominated by solvophobic interactions at all three generations. In contrast, the conformation of the 2-OMe-IPA repeat unit is highly dependent on solvent. This

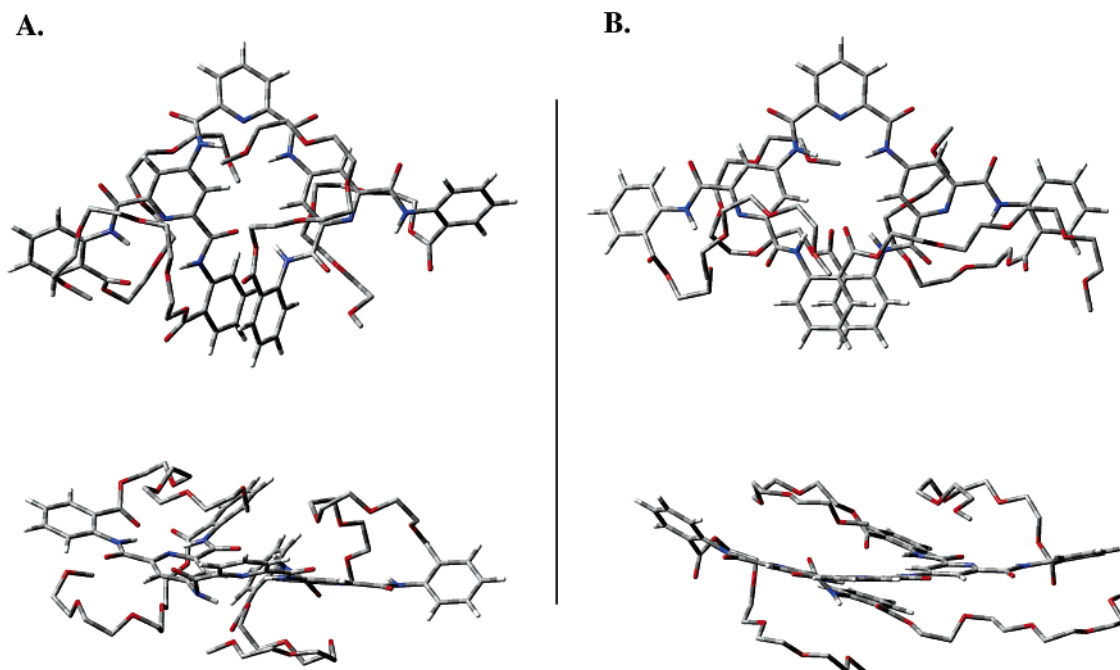


**FIGURE 7.** Comparison of packing of 2,6-pydic dendron **15** in CHCl<sub>3</sub> (A) and DMSO (B) for representative conformers (top: side-on view, bottom: end-on view). Hydrogens of the end chains have been hidden for clarity.



affords a differential effect of solvent on the first generation dendron **10** compared with higher generations where solvent compression dominates the  $V_{\text{hyd}}$ . Accordingly, we can conclude that nonspecific solvophobic compression controls the hydrodynamic properties of both series of dendrons more strongly than solvent-dependent shifts in the conformational equilibria of the repeat units.

In conclusion, dendrons based on 2-methoxyisophthalamides adopt a compact conformation similar to related dendrons based on pyridine-2,6-dicarboxamide. Whereas pyridine-2,6-dicarboxamides and 2-methoxyisophthalamides exhibit qualitatively similar *syn-syn* preferences, a comparison of the conformational equilibria exhibited by both systems reveals subtle differences: (1) 2-OMe-IPA exhibits a lower *syn-syn* preference than 2,6-pyridic and a flatter energetic profile. (2) The *syn-syn* preference of the 2-OMe-IPA branched repeat unit is stabilized entirely by intramolecular hydrogen-bonding interactions. In contrast, the *syn-syn* preference of 2,6-pyridic is a consequence of intramolecular hydrogen-bonding and dipole minimization effects. (3) Polar solvents decrease the *syn-syn* preference of the first generation 2-OMe-IPA dendron more appreciably as compared with the corresponding 2,6-pyridic dendron. These differences in local conformational equilibria are dominated by solvophobic solvent interactions at the global structural level and therefore exhibit compact volumes with similar solvent dependencies.

## Experimental Section

**(2-{2-[2-(2-Methoxyethoxy)ethoxy]ethoxy}ethyl)-2-aminobenzoate (9).** Methyl tetra(ethyleneglycol) (10.00 g, 48.06 mmol), isatoic anhydride (8.23 g, 50.47 mmol, 105 mol %), and *N,N*-(dimethylamino)pyridine (1.17 g, 9.62 mmol, 20 mol %) were added to a dry 250 mL round-bottomed flask fitted with a stir bar. Dioxane (100 mL) was added to dissolve the reagents, and then activated 4 Å molecular sieves were added and the flask was heated to 75 °C. After 48 h, the sieves were filtered, and the solvent was evaporated in vacuo (40 mmHg) affording a brown oil. Purification by flash chromatography (SiO<sub>2</sub>) with 1:1 CH<sub>2</sub>Cl<sub>2</sub>/diethyl ether gave the product as a light yellow oil (15.70 g, 88%): <sup>1</sup>H NMR (250 MHz, CDCl<sub>3</sub>) δ 3.36 (s, 3H), 3.53 (m, 2H), 3.60–3.68 (m, 10H), 3.80 (t, *J* = 4.0 Hz, 2H), 4.41 (t, *J* = 4.0 Hz, 2H), 5.70 (br s, 2H), 6.61 (dd, 1H), 6.63 (ddd, 1H), 7.24 (ddd, *J* = 1.4, 7.0, 8.3 Hz, 1H), 7.87 (dd, *J* = 1.6, 8.0 Hz, 1H); <sup>13</sup>C NMR (250 MHz CDCl<sub>3</sub>) δ 59.1, 63.6, 69.4, 70.6, 70.8, 70.9, 72.1, 110.9, 116.3, 116.8, 131.6, 134.3, 150.6, 168.1; IR (solution cell, CDCl<sub>3</sub>) 3505, 3884, 3055, 2889, 1690, 1617, 1590, 1293, 1248, 1162, 1098 br cm<sup>-1</sup>; HRMS (ESI) *m/z* [Na]<sup>+</sup> 350.1557 (calcd for C<sub>16</sub>H<sub>25</sub>NO<sub>6</sub>Na<sup>+</sup> 350.1574).

**NO<sub>2</sub>-[G1] (10).** (2-{2-[2-(2-Methoxyethoxy)ethoxy]ethoxy}ethyl)-2-aminobenzoate **9** (5.27 g, 14.19 mmol, 200 mol %) and DMAP (173 mg, 1.42 mmol, 20 mol %) were dried under vacuum over P<sub>2</sub>O<sub>5</sub> for 8 h. The vacuum was replaced with nitrogen, the reactants were dissolved in a mixture of CH<sub>2</sub>Cl<sub>2</sub> (15 mL) and pyridine (4 mL), and activated 4 Å sieves were added. 2-Methoxy-5-nitroisophthaloyl dichloride, **7<sup>12</sup>** (1.98 g, 7.10 mmol, 100 mol %), was dissolved in CH<sub>2</sub>Cl<sub>2</sub> (5 mL) and was added dropwise via syringe over 2 h to the stirring yellow solution of amine **9** and DMAP, and the solution was stirred for 4 h at room temperature. The sieves were filtered, and the solvent was removed under reduced pressure (40 mmHg) to give an orange oil. Purification by flash chromatography (SiO<sub>2</sub>) with 1.5% methanol/ethyl acetate afforded a clear oil (4.98 g, 82%): <sup>1</sup>H NMR (500 MHz, CDCl<sub>3</sub>) δ 3.26 (s, 6H), 3.41 (m, 4H), 3.55 (m, 20 H), 3.80 (t, *J* = 5.0 Hz, 4H), 4.21 (s, 3H), 4.47 (t, *J* = 4.5 Hz, 4H), 7.21 (td, *J* = 8.0 Hz, 0.5 Hz, 2H), 7.64 (td, *J* = 8.8, 1.6 Hz, 2H), 8.13 (dd, *J* = 8.0, 1.5

Hz, 2H), 8.88 (s, 2H), 8.92 (d, *J* = 8.0 Hz, 2H), 11.95 (s, 2H); <sup>13</sup>C NMR (125 MHz, CDCl<sub>3</sub>) δ 59.0, 63.7, 64.6, 68.9, 70.5, 70.6, 70.6, 70.7, 71.9, 71.9, 116.4, 121.3, 123.6, 128.7, 130.2, 131.2, 134.6, 140.6, 143.0, 160.5, 162.5, 167.7; IR (neat) 3257, 3090, 2877, 1735, 1678, 1606, 1518, 1449, 1349, 1302, 1008; HR-QTOF-ESI-MS *m/z* calcd for C<sub>41</sub>H<sub>53</sub>N<sub>3</sub>O<sub>17</sub>Na (M + Na)<sup>+</sup> 882.3267, found 882.3305.

**NH<sub>2</sub>-[G1]** (4.34 g, 5.05 mmol, 100 mol %) and SnCl<sub>2</sub>·2H<sub>2</sub>O (11.39 g, 50.47 mmol, 1000 mol %) were dissolved in ethyl acetate (50 mL) and methanol (5 mL) and heated at reflux for 3 h. Ethyl acetate (50 mL) and saturated aqueous NaHCO<sub>3</sub> (100 mL) were added to the cooled solution resulting in the formation of a white precipitate. The precipitate was removed by filtration through a pad of Celite, and the filtrate was poured into a separatory funnel and extracted with ethyl acetate (3 × 100 mL). The combined organic layers were dried (MgSO<sub>4</sub>), and the solvent was removed under reduced pressure (40 mmHg) affording a yellow oil. Purification by flash chromatography (SiO<sub>2</sub>) with 5% methanol/ethyl acetate gave the product as a clear oil (3.87 g, 92%): <sup>1</sup>H NMR (400 MHz, CDCl<sub>3</sub>) δ 3.33 (s, 6H), 3.48 (m, 4H), 3.62 (m, 20H), 3.78 (t, *J* = 4.8 Hz, 4H), 3.88 (s, 3H), 4.00 (s, 2H), 4.45 (t, *J* = 4.4 Hz, 4H), 7.12 (td, *J* = 8.0, 0.8 Hz, 2H), 7.33 (s, 2H), 7.57 (td, *J* = 8.8, 1.6 Hz, 2H), 8.07 (dd, *J* = 8.0, 1.6 Hz, 2H), 8.81 (dd, *J* = 8.4, 1.2 Hz) 11.72 (s, 2H); <sup>13</sup>C NMR (100 MHz, CDCl<sub>3</sub>) δ 59.9, 64.1, 64.3, 68.9, 70.4, 70.5, 70.6, 70.6, 71.8, 116.7, 119.5, 121.6, 123.0, 130.2, 131.1, 134.2, 140.8, 143.3, 148.1, 164.5, 167.2; IR (neat) 3446, 3357, 3261, 2874, 1926, 1679, 1502, 1519, 1446, 1269, 1113; HR-QTOF-ESI-MS *m/z* calcd for C<sub>41</sub>H<sub>55</sub>N<sub>3</sub>O<sub>15</sub>Na (M + Na)<sup>+</sup> 852.3531, found 852.3455.

**NO<sub>2</sub>-[G2] (11).** Following the procedure for preparation of NO<sub>2</sub>-[G1] (**10**), NH<sub>2</sub>-[G1] (2.90 g, 3.49 mmol, 200 mol %), DMAP (43 mg, 0.35 mmol, 20 mol %), and 2-methoxy-5-nitroisophthaloyl dichloride (0.490 g, 1.75 mmol, 100 mol %) were reacted in CH<sub>2</sub>Cl<sub>2</sub> (10 mL) and pyridine (1 mL) to afford NO<sub>2</sub>-[G2] (**11**) as a light yellow oil (2.72 g, 85%) after purification by flash chromatography (SiO<sub>2</sub>) (100:20:4 CHCl<sub>3</sub>/acetone/ethanol): <sup>1</sup>H NMR (250 MHz, CDCl<sub>3</sub>) δ 3.33 (d, 12H), 3.49–3.67 (m, 48H), 3.81 (t, *J* = 5.0 Hz, 8H), 4.04 (s, 6H), 4.22 (s, 3H), 4.48 (t, *J* = 4.5 Hz, 8H), 7.61 (td, *J* = 7.3, 0.75 Hz, 4H), 7.56 (t, *J* = 7.0 Hz, 4H), 8.10 (dd, *J* = 8.0, 1.5 Hz, 4H), 8.44 (s, 4H), 8.82 (d, *J* = 8.25 Hz, 4H), 8.86 (s, 2H), 9.69 (s, 2H), 11.81 (s, 4H); <sup>13</sup>C NMR (125 MHz, CDCl<sub>3</sub>) δ 58.9, 58.9, 64.1, 64.1, 64.5, 68.9, 70.4, 70.4, 70.5, 70.5, 70.6, 71.8, 71.9, 116.6, 121.4, 123.2, 125.4, 128.7, 129.2, 130.1, 131.1, 134.1, 134.3, 140.6, 143.1, 152.7, 160.1, 161.6, 163.8, 167.4; IR (neat) 3509, 3262, 3087, 2875, 2359, 2245, 1681, 1604, 1519, 1447 cm<sup>-1</sup>; MS (MALDI-TOF) for C<sub>91</sub>H<sub>113</sub>N<sub>7</sub>O<sub>35</sub> calcd 1886.73, obsd 1886.85.

**NH<sub>2</sub>-[G2]** (**11**) (2.03 g, 1.09 mmol, 100 mol %) was reduced with SnCl<sub>2</sub>·2H<sub>2</sub>O (2.46 g, 10.91 mmol, 1000 mol %) in ethyl acetate (9 mL) and methanol (1 mL) at reflux for 3 h. Purification by flash chromatography (SiO<sub>2</sub>) (100:20:4 CHCl<sub>3</sub>/acetone/ethanol) afforded the amine as a clear oil (1.03 g, 94%): <sup>1</sup>H NMR (400 MHz, CDCl<sub>3</sub>) δ 3.35 (s, 12H), 3.53 (m, 8H), 3.60–3.69 (m, 40H), 3.83 (t, *J* = 4.4 Hz, 8H), 4.01 (s, 3H), 4.31 (s, 6H), 4.47 (t, *J* = 4.0 Hz, 8H), 7.16 (t, *J* = 7.2 Hz, 4H), 7.16 (buried s, 2H), 7.59 (t, *J* = 7.6 Hz), 8.11 (dd, *J* = 8.0 Hz, 1.2 Hz, 4H), 8.41 (s, 4H), 8.84 (d, *J* = 8.4 Hz, 4H), 9.65 (s, 2H), 11.84 (s, 4H); <sup>13</sup>C NMR (62.5 MHz, CDCl<sub>3</sub>) δ 58.9, 64.1, 64.3, 64.4, 68.9, 70.4, 70.5, 70.5, 70.6, 71.8, 116.5, 120.1, 121.4, 123.0, 125.1, 126.1, 130.3, 131.0, 134.3, 134.6, 140.9, 144.4, 147.0, 152.3, 163.1, 164.0, 167.4; IR (neat), 3451, 3259, 2888, 1959, 1504, 966 cm<sup>-1</sup>; MS (MALDI-TOF) for C<sub>91</sub>H<sub>115</sub>N<sub>7</sub>O<sub>3</sub> calcd 1856.75, obsd 1857.03.

**NO<sub>2</sub>-[G3] (12).** Following the procedure for preparation of NO<sub>2</sub>-[G1] (**10**), NH<sub>2</sub>-[G2] (0.675 g, 0.362 mmol, 200 mol %), DMAP (4.4 mg, 0.036 mmol, 20 mol %), and 2-methoxy-5-nitroisophthaloyl dichloride (0.490 g, 1.75 mmol, 100 mol %) were reacted in CH<sub>2</sub>Cl<sub>2</sub> (1 mL) and pyridine (0.1 mL) to afford NO<sub>2</sub>-[G3] (**12**) as a light yellow oil (0.514 g, 73%) after purification by flash chromatography (SiO<sub>2</sub>) (100:40:8 CHCl<sub>3</sub>/acetone/ethanol): <sup>1</sup>H



NMR (500 MHz, CDCl<sub>3</sub>)  $\delta$  3.35 (s, 24H), 3.46 (m, 16H), 3.52–3.63 (m, 80H), 3.75 (br s, 12H), 3.98 (s, 12H), 4.04 (s, 6H), 4.24 (s, 3H), 4.27 (br s, 16H), 7.07 (t,  $J = 7.5$  Hz, 8H), 7.51 (t,  $J = 7.0$  Hz, 8H), 8.03 (d,  $J = 7.5$  Hz, 8H), 8.40 (br s, 12H), 8.63 (s, 2H), 8.74 (d,  $J = 8.0$  Hz, 8H), 9.78 (s, 4H), 9.94 (s, 2H), 11.82 (s, 8H); <sup>13</sup>C NMR (125 MHz, CDCl<sub>3</sub>)  $\delta$  58.2, 58.9, 64.1, 64.3, 64.5, 68.9, 70.4, 70.5, 70.5, 70.6, 71.8, 116.5, 121.4, 123.1, 125.1, 128.9, 129.9, 131.0, 134.3, 134.7, 140.7, 152.0, 152.3, 162.8, 163.9, 167.4; IR (thin film) 3303, 2876, 1676, 1586, 1519, 1467, 1300, 1256, 1108 cm<sup>-1</sup>; MS (MALDI-TOF) for C<sub>191</sub>H<sub>233</sub>N<sub>15</sub>O<sub>71</sub> calcd 3897.95, obsd 3897.30.

**Synthesis of (R)-O<sub>2</sub>N-[G1] (13). A. ((1R)-2-Methoxy-1-methylethyl)-2-nitrobenzoate.** 2-Nitrobenzoyl chloride (3.24 g, 17.5 mmol, 100 mol %) was dissolved in CH<sub>2</sub>Cl<sub>2</sub> (10 mL) and pyridine (3 mL) in a 50 mL round-bottomed flask. (R)-1-Methoxy-2-propanol (1.58 g, 1.71 mL, 17.5 mmol, 100 mol %) was added dropwise via syringe, and the resulting clear orange solution was stirred at room temperature for 12 h. The solvent was evaporated to give a crude orange oil which was purified by flash chromatography (SiO<sub>2</sub>) with 2:1 hexanes/ethyl acetate to give a clear oil (3.77 g, 90%): <sup>1</sup>H NMR (400 MHz, CDCl<sub>3</sub>)  $\delta$  1.38 (d,  $J = 6.5$  Hz, 3H), 3.40 (s, 3H), 3.50 (dd,  $J = 10.6, 4.1$  Hz, 1H), 3.55 (dd,  $J = 10.6, 6.0$  Hz, 1H), 5.34 (dq,  $J = 6.5, 6.5$  Hz, 1H), 7.62 (td,  $J = 7.8, 1.6$  Hz, 1H), 7.68 (td,  $J = 7.5, 1.3$  Hz, 1H), 7.75 (dd,  $J = 7.5, 1.6$  Hz, 1H), 7.93 (dd,  $J = 7.9, 1.3$  Hz, 1H); <sup>13</sup>C NMR (100 MHz, CDCl<sub>3</sub>)  $\delta$  16.4, 59.5, 72.1, 74.9, 124.2, 128.3, 130.2, 132.0, 133.3, 148.4, 165.3; IR (CDCl<sub>3</sub>) 2990, 2934, 1731, 1537, 1352, 1294, 1257, 1111 cm<sup>-1</sup>; MS (ESI) for C<sub>11</sub>H<sub>13</sub>NO<sub>3</sub>Na<sup>+</sup> calcd 262.0685, obsd 262.0684.

**B. ((1R)-2-Methoxy-1-methylethyl)-2-aminobenzoate.** ((1R)-2-Methoxy-1-methylethyl)-2-nitrobenzoate (2.50 g, 10.45 mmol, 100 mol %) was dissolved in ethyl acetate (40 mL), methanol (20 mL), and Pd–C (0.250 g, 10 mol %). The solution was flushed with N<sub>2</sub> (g), and an H<sub>2</sub> (g) balloon was attached, flushing the solution with H<sub>2</sub> three times. The solution was stirred for 24 h at room temperature, and then it was filtered through Celite to remove the Pd–C. The solvent was removed under reduced pressure (40 mmHg) to give a pink oil. Purification by flash column chromatography (SiO<sub>2</sub>) 5:1 hexanes/ethyl acetate gave the product as a white solid (1.99 g, 91%): mp 60–63 °C; <sup>1</sup>H NMR (400 MHz, CDCl<sub>3</sub>)  $\delta$  1.26 (d,  $J = 6.4$  Hz, 3H), 3.31 (s, 3H), 3.41 (dd,  $J = 4.2, 10.5$  Hz, 1H), 3.49 (dd,  $J = 6.1, 10.5$  Hz, 1H), 5.20 (dq,  $J = 4.2, 6.1, 6.5$  Hz, 1H), 5.62 (bs, 2H), 6.54 (m, 2H), 7.16 (td,  $J = 1.0, 7.3$  Hz, 1H), 7.79 (dd,  $J = 1.0, 7.7$  Hz, 1H); <sup>13</sup>C NMR (100 MHz, CDCl<sub>3</sub>)  $\delta$  17.2, 59.6, 69.6, 75.6, 111.6, 116.6, 117.1, 131.7, 134.4, 150.9, 167.9; IR (solution cell, CHCl<sub>3</sub>) 3504, 3381, 2934, 1686, 1615, 1589, 1560, 1487, 1292, 1247, 1160; MS (ESI) for C<sub>11</sub>H<sub>15</sub>NO<sub>3</sub>Na<sup>+</sup> calcd 232.0944, obsd 232.0940.

**C. [G1] NO<sub>2</sub>.** ((1R)-2-Methoxy-1-methylethyl)-2-aminobenzoate (0.200 g, 0.96 mmol, 200 mol %) and DMAP (0.021 g, 0.17 mmol, 35 mol %) were dried under vacuum over P<sub>2</sub>O<sub>5</sub> for 8 h. The vacuum was replaced with nitrogen, the reactants were dissolved in a mixture of CH<sub>2</sub>Cl<sub>2</sub> (2 mL) and pyridine (1 mL), and activated 4 Å sieves were added. 2-Methoxy-5-nitroisophthaloyl dichloride (0.133 g, 0.48 mmol, 100 mol %) was dissolved in CH<sub>2</sub>Cl<sub>2</sub> (1 mL) and added dropwise via syringe over 2 h to the stirring yellow solution of amine and DMAP, and the solution was stirred for an additional 4 h at room temperature. The sieves were removed by filtration, and the solvent was evaporated under reduced pressure to give an orange oil. Purification by flash chromatography (SiO<sub>2</sub>) with a gradient of 3:1 to 1:1 hexanes/ethyl acetate gave the product as a clear oil (0.175 g, 58%): <sup>1</sup>H NMR (400 MHz, CDCl<sub>3</sub>)  $\delta$  1.28 (d,  $J = 6.44$  Hz, 6H), 3.37 (s, 6H), 3.50 (dd,  $J = 10.6, 3.92$  Hz), 3.58 (dd,  $J = 10.7, 6.4$  Hz, 2H), 4.20 (s, 3H), 5.34 (m, 2H), 7.21 (ddd,  $J = 8.27, 7.10, 1.11$  Hz, 2H), 7.65 (ddd,  $J = 8.70, 7.52, 1.61$  Hz, 2H), 8.12 (dd,  $J = 8.0, 1.56$  Hz, 2H), 8.85 (obscured d, 2H), 8.88 (s, 2H), 11.99 (s, 2H); <sup>13</sup>C NMR (100 MHz, CDCl<sub>3</sub>)  $\delta$  16.7, 59.6, 64.0, 71.0, 75.3, 117.2, 121.7, 124.0, 129.0, 130.6, 131.5, 134.9, 141.0, 143.4, 160.9, 193.0, 167.6; IR (CH<sub>2</sub>Cl<sub>2</sub>) 3261, 2988, 2886, 1681,

1606, 1517, 1453, 1348, 1305; MS (ESI) for C<sub>30</sub>H<sub>31</sub>N<sub>3</sub>O<sub>11</sub>Na<sup>+</sup> calcd 632.1850, obsd 632.1839.

**D. H<sub>2</sub>N-[G1] (13).** [G1] NO<sub>2</sub> (90 mg, 0.143 mmol) was dissolved in ethyl acetate (30 mL) and methanol (10 mL). Pd/C (10%, 0.014 g, 0.2 mmol) was added to the solution, and the mixture was hydrogenated at 1 atm of H<sub>2</sub> pressure for 48 h. The catalyst was removed by filtration through a pad of Celite and rinsed with ethyl acetate (30 mL). The solvent was removed under reduced pressure (40 mmHg) to give a clear yellow oil. Purification by flash column chromatography (SiO<sub>2</sub>) using 1:1 hexanes/ethyl acetate gave the product (0.060 g, 88%) as a white solid: mp 71–73 °C; <sup>1</sup>H NMR (400 MHz, CDCl<sub>3</sub>)  $\delta$  1.34 (d,  $J = 6.48$  Hz, 6H), 3.35 (s, 6H), 3.49 (dd,  $J = 4.04, 10.6$  Hz, 2H), 3.56 (dd,  $J = 10.6, 6.3$  Hz, 2H), 3.92 (s, 3H), 5.34 (m, 2H), 7.14 (ddd,  $J = 8.16, 6.96, 1.08$  Hz, 2H), 7.37 (s, 2H), 7.58 (ddd,  $J = 8.68, 7.48, 1.6$  Hz, 2H), 8.07 (dd,  $J = 7.96, 1.56$  Hz, 2H), 8.82 (dd,  $J = 8.28, 0.44$  Hz, 2H), 11.79 (s, 2H); <sup>13</sup>C NMR (100 MHz, CDCl<sub>3</sub>)  $\delta$  14.5, 59.5, 64.5, 70.7, 75.3, 117.6, 120.1, 122.0, 123.3, 130.7, 131.3, 134.4, 141.2, 143.2, 148.8, 165.0, 167.2; IR (CDCl<sub>3</sub>) 3511, 3254, 3187, 2863, 2455, 2375, 1661, 1624, 1520, 1426; MS (ESI) for C<sub>31</sub>H<sub>35</sub>N<sub>3</sub>O<sub>9</sub>Na<sup>+</sup> calcd 616.2265, obsd 616.2278.

**Cl-[G1] (14).** A solution of 4-chloropyridine-2,6-dicarbonyl dichloride (1.57 g, 6.57 mmol) in CH<sub>2</sub>Cl<sub>2</sub> (4.5 mL) was added to a solution of (2-{2-[2-(2-methoxyethoxy)ethoxy]ethoxy}ethyl)-2-aminobenzoate (9) (4.30 g, 13.13 mmol) and 4 Å molecular sieves (2 g) in pyridine (8.7 mL) and CH<sub>2</sub>Cl<sub>2</sub> (17.5 mL) over 1 h at room temperature. After 16 h at room temperature, the solvents were evaporated in vacuo, and the resultant residue was suspended in CH<sub>2</sub>Cl<sub>2</sub> and purified by flash chromatography (SiO<sub>2</sub>) with 10% Et<sub>2</sub>O/CH<sub>2</sub>Cl<sub>2</sub> to 50% Et<sub>2</sub>O/CH<sub>2</sub>Cl<sub>2</sub> to 100% MeOH/CH<sub>2</sub>Cl<sub>2</sub> to afford the product as a clear yellow oil (5.31 g, 99%):  $R_f$  (EtOAc) 0.13;  $R_f$  (5% MeOH/EtOAc) 0.34;  $R_f$  (10% MeOH/EtOAc) 0.42; <sup>1</sup>H NMR (400 MHz, CDCl<sub>3</sub>)  $\delta$  3.34 (s, 6H), 3.49–3.52 (m, 8H), 3.54–3.62 (m, 20H), 4.18 (dd,  $J = 4.8$  Hz, 4H), 7.20 (ddd,  $J = 1.0, 8.2, 8.2$  Hz, 2H), 7.63 (ddd,  $J = 1.6, 8.6, 8.6$  Hz, 2H), 8.10 (dd,  $J = 1.5, 8.0$  Hz, 2H), 8.41 (s, 2H, pyr), 8.72 (dd,  $J = 0.6, 8.3$  Hz, 2H), 12.63 (s, 2H); <sup>13</sup>C NMR (100 MHz, CDCl<sub>3</sub>)  $\delta$  59.2, 64.4, 69.0, 70.6, 70.7, 72.1, 117.9, 121.8, 123.9, 125.7, 131.4, 134.6, 140.1, 148.4, 150.9, 161.2, 167.2; IR (CHCl<sub>3</sub>) 3356, 3254, 3089, 2883, 1685, 1606, 1582, 1534, 1454, 1308, 1261, 1086 cm<sup>-1</sup>; HRMS (ESI)  $m/z$  [M + Na]<sup>+</sup> 842.2891 (calcd 842.2874 for C<sub>39</sub>H<sub>50</sub>ClN<sub>3</sub>O<sub>14</sub>Na<sup>+</sup>).

**NH<sub>2</sub>-[G1].** A suspension of Cl-[G1] (14) (5.31 g, 6.47 mmol) and sodium azide (8.42 g, 129.44 mol) in DMF (13 mL) was heated to 75 °C for 4.5 h. The solvent was evaporated in vacuo, suspended in EtOAc, and filtered through a pad of Celite. The filtrate was evaporated affording N<sub>3</sub>-[G1] as an orange oil that was used without further purification (5.33 g, quantitative);  $R_f$  (5% MeOH/EtOAc) 0.34; <sup>1</sup>H NMR (400 MHz, CDCl<sub>3</sub>)  $\delta$  3.35 (s, 6H), 3.52 (m, 8H), 3.60 (m, 20H), 4.20 (dd,  $J = 4.8$  Hz, 4H), 7.20 (dt,  $J = 1.0, 7.6$  Hz, 2H), 7.65 (dt,  $J = 1.5, 7.8$  Hz, 2H), 8.07 (s, 2H, pyr), 8.11 (dd,  $J = 1.5, 8.0$  Hz, 2H), 8.74 (dd,  $J = 1.0, 8.3$  Hz, 2H), 12.66 (s, 2H); IR (thin film) 3355, 3245, 2876, 1686 cm<sup>-1</sup>; HRMS (ESI)  $m/z$  [M + Na]<sup>+</sup> 849.3277 (calcd 849.3277 for C<sub>39</sub>H<sub>50</sub>N<sub>6</sub>O<sub>14</sub>Na<sup>+</sup>). A degassed suspension of the crude N<sub>3</sub>-[G1] (5.35 g, 6.47 mmol) and 10% Pd on carbon (0.53 g) in EtOAc (32 mL) was pressurized to 50 psi using a Parr hydrogenator, and the mixture was shaken for 13 h. The solution was filtered over Celite, and the solids were rinsed with EtOAc (300 mL). The resultant filtrate was evaporated giving a light yellow solid that was purified using flash chromatography (SiO<sub>2</sub>) with 5% MeOH/EtOAc affording the amine as a white gummy solid (4.69 g, 91%): mp 47–49 °C (CH<sub>2</sub>Cl<sub>2</sub>);  $R_f$  (5% MeOH/EtOAc) 0.27;  $R_f$  (10% MeOH/EtOAc) 0.47;  $R_f$  (5% MeOH/CH<sub>2</sub>Cl<sub>2</sub>) 0.33; <sup>1</sup>H NMR (400 MHz, CDCl<sub>3</sub>)  $\delta$  3.32 (s, 6H), 3.42 (br m, 12H), 3.58 (br m, 16H), 4.18 (br dd,  $J = 4.3, 4.9$  Hz, 4H), 5.26 (br s, 2H), 7.18 (ddd,  $J = 1.1, 7.3, 8.0$  Hz, 2H), 7.62 (obs ddd,  $J = 1.4, 7.4, 8.5$  Hz, 2H), 7.58 (obs s, 2H), 8.04 (dd,  $J = 1.5, 8.0$  Hz, 2H), 8.64 (dd,  $J = 0.9, 8.4$  Hz, 2H), 12.46 (s, 2H); <sup>13</sup>C NMR (100 MHz, CDCl<sub>3</sub>)  $\delta$  59.0, 64.4, 68.9, 70.5, 70.6, 72.0,

110.1, 118.2, 121.8, 123.4, 131.4, 134.2, 140.2, 150.0, 156.6, 163.0, 167.2; IR (CHCl<sub>3</sub>) 3518, 3420, 3350, 3248, 1683 cm<sup>-1</sup>; HRMS (ESI) *m/z* [M + Na]<sup>+</sup> 823.3372 (calcd 823.3372 for C<sub>39</sub>H<sub>52</sub>N<sub>4</sub>O<sub>14</sub>Na).

**Cl-[G2] (15).** Following the procedure for preparation of Cl-[G1] (**14**), 4-chloropyridine-2,6-dicarbonyl dichloride (0.23 g, 0.95 mmol), NH<sub>2</sub>-[G1] (1.37 g, 1.71 mmol), DMAP (58 mg, 0.38 mmol), and pyridine (0.30 g, 0.31 mL, 3.80 mmol) were reacted in THF (2 mL) at room temperature for 72 h affording Cl-[G2] **15** following purification by flash chromatography (SiO<sub>2</sub>) with 10% MeOH/EtOAc to 5% MeOH/CH<sub>2</sub>Cl<sub>2</sub>) as an off-white solid (0.73 g, 48%): mp 79–84 °C (CH<sub>2</sub>Cl<sub>2</sub>); *R<sub>f</sub>* (10% MeOH/EtOAc) 0.06; *R<sub>f</sub>* (5% MeOH/CH<sub>2</sub>Cl<sub>2</sub>) 0.38; <sup>1</sup>H NMR (400 MHz, DMSO-*d*<sub>6</sub>) δ 3.18 (s, 12), 3.36 (m, 16H), 3.44 (obs m, 32H), 3.60 (br s, 8H), 4.15 (br s, 8H), 7.25 (dd, *J* = 7.2 Hz, 4H), 7.67 (dd, *J* = 7.0 Hz, 4H), 8.01 (d, *J* = 7.6 Hz, 4H), 8.21 (s, 2H), 8.57 (d, *J* = 8.0 Hz, 4H), 8.90 (s, 4H), 11.50 (s, 2H), 12.39 (s, 4H); <sup>13</sup>C NMR (100 MHz, DMSO-*d*<sub>6</sub>) δ 58.0, 64.1, 67.9, 69.6, 69.6, 69.7, 69.8, 71.2, 114.9, 117.6, 121.0, 123.8, 126.0, 130.9, 134.3, 139.2, 146.8, 148.6, 149.2, 149.5, 161.2, 161.4, 166.4; IR (thin film) 3510, 3314, 3248, 1710, 1692, 1680 cm<sup>-1</sup>; HRMS (ES) *m/z* [Na]<sup>+</sup> 1788.6434 (calcd 1788.6470 for C<sub>85</sub>H<sub>104</sub>ClN<sub>9</sub>O<sub>30</sub>Na).

**NH<sub>2</sub>-[G2]. A. N<sub>3</sub>-[G2].** Cl-[G2] **15** (0.200 g, 0.113 mmol, 100 mol %) and NaN<sub>3</sub> (0.074 g, 1.13 mmol, 1000 mol %) were stirred in dry DMF (5 mL) at 70 °C for 10 h. The DMF was evaporated under reduced pressure (1 mmHg) to give a crude orange solid. Purification by flash chromatography (SiO<sub>2</sub>) with 100:40:8 chloroform/acetone/ethanol gave N<sub>3</sub>-[G2] as a clear oil (0.190 g, 95%): <sup>1</sup>H NMR (500 MHz, DMSO-*d*<sub>6</sub>) δ 3.18 (s, 12H), 3.38–3.46 (m, 48H), 3.59 (t, *J* = 5.25 Hz, 8H), 4.16 (t, *J* = 3.75 Hz, 8H), 7.34 (t, *J* = 8.0 Hz, 4H), 7.78 (t, *J* = 8.25 Hz, 4H), 8.07 (d, *J* = 8.0 Hz, 4H), 8.31 (s, 2H), 8.67 (d, *J* = 8.25 Hz, 4H), 9.08 (s, 4H), 11.74 (s, 2H), 12.53 (s, 4H)<sup>1</sup>MS (MALDI-TOF) for C<sub>85</sub>H<sub>104</sub>N<sub>12</sub>O<sub>30</sub>Na<sup>+</sup> calcd 1796.80, obsd 1796.59.

**B. NH<sub>2</sub>-[G2].** N<sub>3</sub>-[G2] (0.20 g, 0.113 mmol, 100 mol %) was dissolved in ethyl acetate (10 mL) and methanol (5 mL) in a hydrogenation jar. The solution was purged with N<sub>2</sub> for 15 min, and Pd–C (0.0010 g, 10 mol %) was added. The solution was placed under H<sub>2</sub> (50 psi) on a Parr hydrogenator for 12 h. The Pd–C was removed by filtration, and the solvent was evaporated under reduced pressure (40 mmHg) to give a crude yellow oil. Purification by flash chromatography (SiO<sub>2</sub>) with 100:40:8 chloroform/acetone/ethanol gave the product as a clear oil (0.190 g, 97%): <sup>1</sup>H NMR (500 MHz, DMSO) δ 3.18 (s, 12H), 3.39 (t, *J* = 2.8 Hz, 8H), 3.42–3.45 (m, 40H), 3.58 (t, *J* = 3.6 Hz, 8H), 4.16

(t, *J* = 4.5 Hz, 8H), 7.09 (s, 2H), 7.33 (t, *J* = 8.0 Hz, 4H), 7.63 (s, 2H), 7.76 (td, *J* = 8.25 Hz, 1.0 Hz, 4H), 8.06 (dd, *J* = 8.0 Hz, 1.0 Hz, 4H), 8.66 (d, *J* = 8.0 Hz, 4H), 9.09 (s, 4H), 11.62 (s, 2H), 12.52 (s, 4H); <sup>13</sup>C NMR (125 MHz, DMSO-*d*<sub>6</sub>) δ 58.4, 64.6, 68.3, 70.0, 70.1, 70.1, 70.2, 71.7, 110.7, 115.5, 118.3, 121.7, 124.4, 131.5, 134.9, 139.6, 148.9, 149.6, 150.1, 157.7, 162.0, 164.3, 167.0; IR (CDCl<sub>3</sub>) 3526, 3439, 3310, 3241, 1687 cm<sup>-1</sup>; MS (MALDI-TOF) for C<sub>85</sub>H<sub>106</sub>N<sub>10</sub>O<sub>30</sub>Na<sup>+</sup> calcd 1769.71, obsd 1769.71.

**Cl-[G3] (16).** Following the procedure for preparation of Cl-[G1] (**14**), 4-chloropyridine-2,6-dicarbonyl dichloride (0.093 g, 0.0039 mmol, 100 mol %), NH<sub>2</sub>-[G2] (0.136 g, 0.078 mmol, 200 mol %), and DMAP (0.0010 g, 0.0078 mmol, 20 mol %) were reacted at room temperature in a mixture of CH<sub>2</sub>Cl<sub>2</sub> (0.5 mL) and pyridine (0.1 mL) in the presence of 4 Å molecular sieves (0.2 g). Purification by flash chromatography (SiO<sub>2</sub>) with 10:1 CH<sub>2</sub>Cl<sub>2</sub>/methanol gave the product as a clear oil (0.101 g, 70%): <sup>1</sup>H NMR (500 MHz, CDCl<sub>3</sub>, 60 °C) δ 3.22 (s, 24H), 3.40 (t, *J* = 4.5 Hz, 16H), 3.44–3.51 (m, 80H), 3.61 (t, *J* = 5.0 Hz, 16H), 4.16 (t, *J* = 4.5 Hz, 16H), 7.25 (t, *J* = 8.0 Hz, 8H), 7.65 (t, *J* = 8.0 Hz, 8H), 8.03 (d, *J* = 7.0 Hz, 8H), 8.22 (s, 2H), 8.59 (d, *J* = 8.0 Hz, 8H), 9.03 (s, 8H), 9.14 (s, 4H), 11.45 (s, 2H), 11.60 (s, 4H), 12.33 (s, 8H); <sup>13</sup>C NMR (125 MHz, CDCl<sub>3</sub>, 60 °C) δ 58.4, 64.5, 68.5, 70.1, 70.2, 70.3, 70.3, 71.8, 115.8, 116.9, 118.6, 121.9, 124.1, 131.3, 134.5, 139.8, 148.7, 149.3, 149.8, 150.2, 161.9, 163.2, 166.9; IR (CHCl<sub>3</sub>) 3329, 3250, 1683 cm<sup>-1</sup>; MS (MALDI-TOF) for C<sub>177</sub>H<sub>212</sub>ClN<sub>21</sub>O<sub>62</sub>Na<sup>+</sup> calcd 3684.13, obsd 3684.45.

**Acknowledgment.** This work was supported by the National Science Foundation (CHE-0239871 and CHE-00526864). Generous allocations of computer time at the Ohio Supercomputer Center are gratefully acknowledged. M.P.D. also acknowledges a Procter and Gamble fellowship.

**Supporting Information Available:** General synthetic methods, setup details for TCSPC and fluorescence studies, SEC characterization of the dendrons, and DOSY <sup>1</sup>H NMR data for dendrons **11**, **12**, **15**, and **16**. Summary of calculated energies, dipole moments, and natural population analyses of all stationary points located for 2-OMe-IPA and 2,6-pydic. Summary of energies, dihedral angles, and molecular volumes of conformers within ~12 kcal/mol of the global minimum for **11** and **15**. Crystal structure data for dendron **13** and a complete ref 8a. This material is available free of charge via the Internet at <http://pubs.acs.org>.

JO061351K